

A Comparison of Hammerstein-Type Nonlinear Models for Identification of Human Response to Virtual 3D Face Stimuli

Vytautas KAMINSKAS*, Aušra VIDUGIRIENĖ

*Department of Systems Analysis, Vytautas Magnus University
Vileikos g. 8, LT-40444, Kaunas, Lithuania
e-mail: v.kaminskas@if.vdu.lt, a.vidugiriene@if.vdu.lt*

Received: January 2016; accepted: May 2016

Abstract. A comparison of two nonlinear input-output models describing the relationship between human emotion (excitement, frustration and engagement/boredom) signals and a virtual 3D face feature (distance-between-eyes) is introduced in this paper. A method of least squares with projection to stability domain for the building of stable models with the least output prediction error is proposed. Validation was performed with seven volunteers, and three types of inputs. The results of the modelling showed relatively high prediction accuracy of excitement, frustration and engagement/boredom signals.

Key words: 3D face, human emotions, Hammerstein-type model, parameter estimation, model validation.

1. Introduction

Virtual environment became a part of our daily life (computer games, learning environments, social networks and their games, work tasks, online shopping, etc.). These environments affect the users in both positive and negative ways. It is important to investigate relations between virtual stimuli and human emotions when interacting with them to prevent users from harmful effects (Calvo *et al.*, 2015; Scherer *et al.*, 2010). Human state observation is an important task for this purpose. Plenty of bio-signals are used for human state monitoring (Suprijanto *et al.*, 2009; Zisook *et al.*, 2013). We use EEG-based signals because of their reliability and quick response (Grimann *et al.*, 2011; Hondrou and Caridakis, 2012; Sourina and Liu, 2011; Tan *et al.*, 2010).

A linear input-output structure models for exploring dependencies between virtual 3D face features and human reaction to them were investigated in Vaškevičius *et al.* (2014). Four reaction signals were used: excitement, meditation, frustration, and engagement/boredom. A dynamical stimulus (virtual 3D face) was characterized by distance-between-eyes, nose-width and chin-width. It was shown that the features of a virtual face

* Corresponding author.

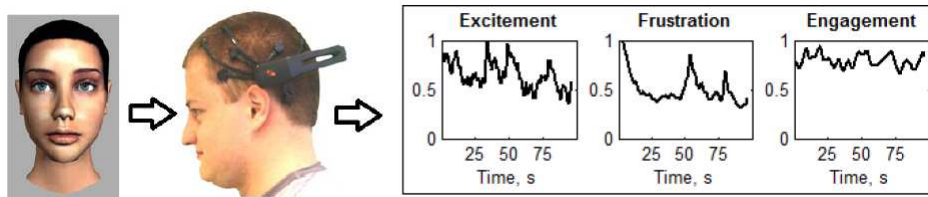


Fig. 1. Input–output scheme for the experiments.

have the largest influence to human excitement, frustration and engagement signals. Then one linear model was modified and two nonlinear models offered in Kaminskas *et al.* (2014) for the modelling of previously mentioned signals as reactions to a virtual dynamic 3D face.

In this investigation we compare two Hammerstein-type nonlinear input-output structure models describing the dependencies between human emotional signals (excitement, frustration and engagement) and a virtual 3D face feature (distance-between-eyes). We show that two nonlinear models used in Kaminskas *et al.* (2014) are piece-wise Hammerstein-type model cases. The data collected from experiments with three different input types are used for model parameters' estimation and validation.

2. Experiment Planning and Observations

A virtual 3D face with changing distance between eyes was used for input as stimulus (shown in a monitor) and EEG-based pre-processed excitement, frustration and engagement signals of a volunteer were measured as output (Fig. 1). The output signals were recorded using Emotiv Epoc device that records EEG inputs from 14 channels (according to international 10–20 locations): AF3, F7, F3, FC5, T7, P7, O1, O2, P8, T8, FC6, F4, F8, AF4, Emotiv Epoc specifications).

Dynamical stimulus was formed from a changing woman's face. One 3D face created with Autodesk MAYA was used as a "neutral" one (Fig. 1, left). Other 3D faces were formed by changing distance-between-eyes in an extreme manner (Figs. 2–4). The smooth and sudden transitions between normal and extreme stages were programmed. There were three input signals used in the experiments.

The first one – TYPE I – (Fig. 2) was formed when a signal of neutral face was equal to 0, the signal of the largest distance-between-eyes was equal to 1.75 and the signal of the smallest distance-between-eyes was equal to -1.75 . The values in-between were changed linearly. Time interval between the largest/smallest value and zero (normal face) was 10 s. The features were changing continuously: from normal to large, then back to normal and to small, then again to normal and to large and again back to normal.

The second input signal – TYPE II – (Fig. 3) was formed as sudden changes between extreme stages. Neutral face's signal was equal to 0, the signal of the largest distance-between-eyes was equal to 1.25 and the signal of the smallest distance-between-eyes was equal to -1.25 . The values in-between were changed suddenly. Time interval between

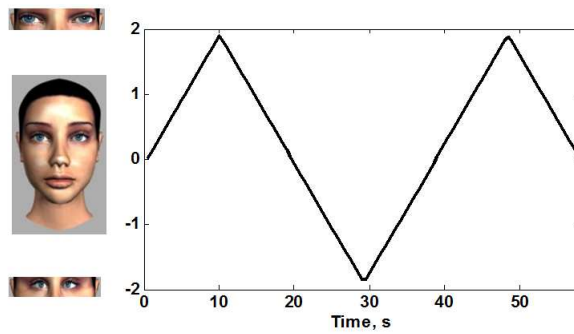


Fig. 2. Input signal TYPE I: experiment plan.

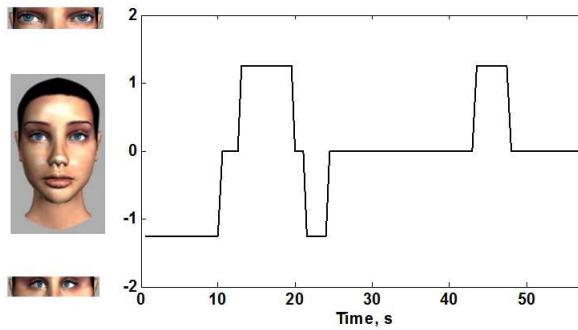


Fig. 3. Input signal TYPE II: experiment plan.

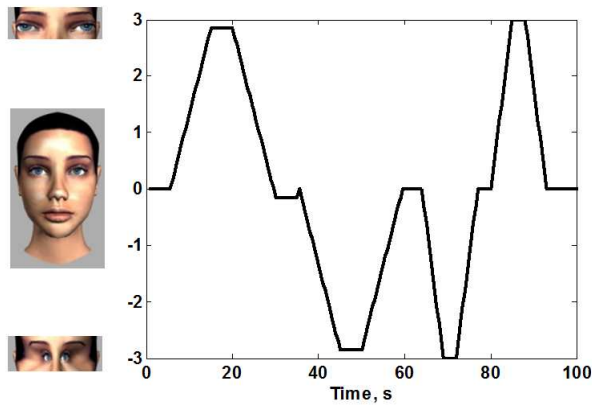


Fig. 4. Input signal TYPE III: experiment plan.

the largest/smallest value and zero (normal face) was from 3 to 20 s. The features were changing from small to normal and then to large, then back to normal and to small, then again to normal and to large and again back to normal.

The third input signal – TYPE III – was formed in a combined manner from previous two (Fig. 4). At first “neutral” face was shown for 5 s, then distance-between-eyes was

increased continuously and in 10 s the largest distance-between-eyes (Fig. 4, top left) was reached, then 5 s of stable face was shown and after that the face came back to “normal” in 10 s. Then “normal” face was shown for 5 s, followed by 10 s long continuous change to the face with smallest distance-between-eyes (Fig. 4, bottom left), again 5 s of stable face was shown and in the next 10 s the face came back to “normal”. Then everything was repeated from the beginning using 3 s time intervals for stable face and 5 s for continuous change. “Neutral” face’s signal has value 0, a signal of the largest distance-between-eyes corresponds to value 3 and a signal of the smallest distance-between-eyes corresponds to value -3 .

Values of the output signals – excitement, frustration, and engagement/boredom – varied from 0 to 1. If excitement, frustration, and engagement are low, the value is close to 0 and if they are high, the value is close to 1. The signals were recorded with the sampling period of $T_0 = 0.5$ s.

3. Building of Hammerstein-Type Models

Dependencies between human emotion signals (excitement, frustration, and engagement/boredom) as reactions to virtual 3D face feature (distance-between-eyes) changes are described by input-output structure Hammerstein-type model (Kaminskas, 1985):

$$y_t = W(z^{-1})f(x_t) + H(z^{-1})\varepsilon_t, \quad (1)$$

where

$$W(z^{-1}) = \frac{B(z^{-1})}{A(z^{-1})}, \quad (2)$$

$$H(z^{-1}) = \frac{1}{A(z^{-1})} \quad (3)$$

are transfer functions of the dynamical channels of the input and the disturbance (Fig. 5), and

$$f(x_t) = f_0 + f_1|x_t| \quad (4)$$

or

$$f(x_t) = f_0 + f_2x_t^2 \quad (5)$$

is a nonlinear characteristics of the input channel (Fig. 5),

$$A(z^{-1}) = 1 + \sum_{i=1}^n a_i z^{-i}, \quad B(z^{-1}) = \sum_{j=0}^m b_j z^{-j} \quad (6)$$

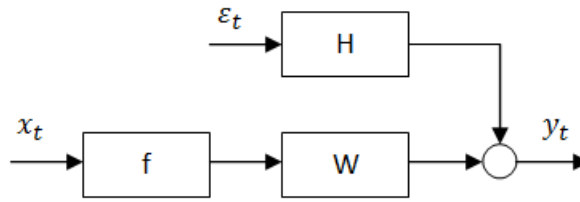


Fig. 5. Hammerstein-type model structure.

are the polynomials of the transfer functions, y_t is an output (excitement, frustration, or engagement/boredom signal), x_t is an input (distance-between-eyes) signal respectively expressed as

$$y_t = y(tT_0), \quad x_t = x(tT_0) \tag{7}$$

with sampling period T_0 , ε_t corresponds to white-noise signal, and z^{-1} is the backward shift operator ($z^{-1}x_t = x_{t-1}$). A sign $| \cdot |$ denotes absolute value.

Equation (1) when using expressions (2)–(6) is changed to the following form:

$$A(z^{-1})y_t = \theta_0 + B_*(z^{-1})f_*(x_t) + \varepsilon_t, \tag{8}$$

where

$$\theta_0 = f_0 \sum_{j=0}^m b_j, \tag{9}$$

$$B_*(z^{-1}) = \sum_{j=0}^m b_j^* z^{-j}, \tag{10}$$

$$b_j^* = f_1 b_j, \quad j = 0, 1, \dots, m \tag{11}$$

or

$$b_j^* = f_2 b_j, \quad j = 0, 1, \dots, m, \tag{12}$$

$$f_*(x_t) = |x_t| \tag{13}$$

or

$$f_*(x_t) = x_t^2. \tag{14}$$

Equations (8)–(14) are equivalent to the nonlinear model equations used in Kamin-skas *et al.* (2014) when $|f_0| > 0$ and $f_1 = f_2 = 1$. So these models are a piece-wise Hammerstein-type model case. Parameters (coefficients of the polynomials), orders (degrees m and n of the polynomials), and constant θ_0 of the models (8)–(14) are unknown.

They have to be estimated according to the observations obtained during the experiments with the volunteers.

Equation (8) can be expressed in the following form:

$$y_t = \theta_0 + \sum_{j=0}^m b_j^* f_*(x_{t-j}) - \sum_{i=1}^n a_i y_{t-i} + \varepsilon_t. \quad (15)$$

It is not difficult to see that (15) can be expressed as the linear regression equation:

$$y_t = \mathbf{d}_t^T \mathbf{c} + \varepsilon_t, \quad (16)$$

where

$$\mathbf{d}_t^T = [1, f_*(x_t), f_*(x_{t-1}), \dots, f_*(x_{t-m}), -y_{t-1}, \dots, -y_{t-n}], \quad (17)$$

and

$$\mathbf{c}^T = [\theta_0, b_0^*, b_1^*, \dots, b_m^*, a_1, a_2, \dots, a_n], \quad (18)$$

T is a vector transpose sign.

For the estimation of unknown parameter vector \mathbf{c} we use a method of least squares with projection to the stability domain (Kaminskas, 1982). Least squares estimates:

$$\hat{\mathbf{c}} = \mathbf{Q}^{-1} \mathbf{q}, \quad (19)$$

where \mathbf{Q} and \mathbf{q} are expressed as follows:

$$\mathbf{Q} = \sum_{t=1}^M \mathbf{d}_t \mathbf{d}_t^T, \quad \mathbf{q} = \sum_{t=1}^M y_t \mathbf{d}_t \quad (20)$$

and M is a number of observation values that are used to build a model.

After calculating the estimates of model parameters, stability condition of a model is verified (Kaminskas, 1982). It means that the roots

$$z_i^A : \hat{A}_M(z) = 0, \quad i = 1, 2, \dots, n \quad (21)$$

of the following polynomial

$$\hat{A}_M(z) = z^n \hat{A}_M(z^{-1}) = z^n + \sum_{i=1}^n \hat{a}_i^M z^{n-i} \quad (22)$$

have to be in the stability domain, i.e. in the unit disk

$$|z_i^A| < 1, \quad i = 1, 2, \dots, n, \quad (23)$$

where \hat{a}_i^M are the least squares estimates of polynomial $A(z^{-1})$ coefficients.

If the condition (23) is not satisfied, coefficients of polynomial $\hat{A}_M(z^{-1})$ are projected

$$\hat{a}_i = \gamma \hat{a}_i^M, \quad 0 < \gamma \leq 1, \quad i = 1, 2, \dots, n, \tag{24}$$

to the stability domain. A calculation of the projection coefficient γ was given in the previous work Kaminskias *et al.* (2014) when $n \leq 2$ (stability domain is defined by linear equations). It is easy to calculate γ constant when $n \leq 3$, because the stability domain is defined by Jury (1962):

$$-1 < \hat{a}_1 < 1, \quad \text{if } n = 1, \tag{25}$$

$$\begin{cases} 1 + \hat{a}_1 + \hat{a}_2 > 0, \\ 1 - \hat{a}_1 + \hat{a}_2 > 0, \\ -1 < \hat{a}_2 < 1, \end{cases} \quad \text{if } n = 2, \tag{26}$$

$$\begin{cases} 1 + \hat{a}_1 + \hat{a}_2 + \hat{a}_3 > 0, \\ 1 - \hat{a}_1 + \hat{a}_2 - \hat{a}_3 > 0, \\ 1 + \hat{a}_1 \hat{a}_3 - \hat{a}_2 - \hat{a}_3^2 > 0, \\ -1 < \hat{a}_3 < 1, \end{cases} \quad \text{if } n = 3. \tag{27}$$

Then using (24) in (25)–(27), we get:

$$\gamma = \min \{1, \gamma_1^{(1)}\}, \quad \text{if } n = 1, \tag{28}$$

$$\gamma_1^{(1)} = \frac{1}{|\hat{a}_1^M|} - \gamma_0, \tag{29}$$

$$\gamma = \min \{1, \gamma_1^{(2)}, \gamma_2^{(2)}, \gamma_3^{(2)}\}, \quad \text{if } n = 2, \tag{30}$$

$$\gamma_1^{(2)} = \begin{cases} -\frac{1}{\hat{a}_1^M + \hat{a}_2^M} - \gamma_0, & \text{if } \hat{a}_1^M + \hat{a}_2^M < 0, \\ 1, & \text{in other cases,} \end{cases} \tag{31}$$

$$\gamma_2^{(2)} = \begin{cases} -\frac{1}{\hat{a}_2^M - \hat{a}_1^M} - \gamma_0, & \text{if } \hat{a}_2^M - \hat{a}_1^M < 0, \\ 1, & \text{in other cases,} \end{cases} \tag{32}$$

$$\gamma_3^{(2)} = \frac{1}{|\hat{a}_2^M|} - \gamma_0, \tag{33}$$

$$\gamma = \min \{1, \gamma_1^{(3)}, \gamma_2^{(3)}, \gamma_3^{(3)}, \gamma_4^{(3)}\}, \quad \text{if } n = 3, \tag{34}$$

$$\gamma_1^{(3)} = \begin{cases} -\frac{1}{\hat{a}_1^M + \hat{a}_2^M + \hat{a}_3^M} - \gamma_0, & \text{if } \hat{a}_1^M + \hat{a}_2^M + \hat{a}_3^M < 0, \\ 1, & \text{in other cases,} \end{cases} \tag{35}$$

$$\gamma_2^{(3)} = \begin{cases} -\frac{1}{\hat{a}_2^M - \hat{a}_1^M - \hat{a}_3^M} - \gamma_0, & \text{if } \hat{a}_2^M - \hat{a}_1^M - \hat{a}_3^M < 0, \\ 1, & \text{in other cases,} \end{cases} \tag{36}$$

$$\gamma_3^{(3)} = \frac{1}{|\hat{a}_3^M|} - \gamma_0, \tag{37}$$

$\gamma_4^{(3)}$ is a smaller solution (from all real positive solutions) of a quadratic equation

$$(\hat{a}_1^M \hat{a}_3^M - (\hat{a}_3^M)^2) \gamma^2 - \hat{a}_2^M \gamma + 1 = 0. \quad (38)$$

Positive constant $\gamma_0 \in [0.001, 0.01]$.

Estimates of the model orders – \hat{m} and \hat{n} – are defined from the following conditions (Kaminskas, 1982):

$$\hat{n} = \min\{\tilde{n}\}, \quad \hat{m} = \min\{\tilde{m}\}, \quad (39)$$

where \tilde{m} and \tilde{n} are polynomial (6) degrees when the following inequalities are correct:

$$\left| \frac{\sigma_\varepsilon[m, n+1] - \sigma_\varepsilon[m, n]}{\sigma_\varepsilon[m, n]} \right| \leq \delta, \quad n = 1, 2, \dots, \quad (40)$$

$$\left| \frac{\sigma_\varepsilon[m+1, n] - \sigma_\varepsilon[m, n]}{\sigma_\varepsilon[m, n]} \right| \leq \delta, \quad m = 1, 2, \dots, n, \quad (41)$$

where

$$\sigma_\varepsilon[m, n] = \sqrt{\frac{1}{N} \sum_{t=1}^N \hat{\varepsilon}_t^2[m, n]} \quad (42)$$

is one-step-ahead output prediction error standard deviation,

$$\hat{\varepsilon}_t[m, n] = y_t - \hat{y}_{t|t-1}[m, n] \quad (43)$$

is one-step-ahead output prediction error,

$$\hat{y}_{t|t-1}[m, n] = \hat{\theta}_0 + z[1 - \hat{A}(z^{-1})]y_{t-1} + \hat{B}_*(z^{-1})f_*(x_t) \quad (44)$$

is one-step-ahead output prediction (Kaminskas, 1982), z is the forward shift operator ($zy_t = y_{t+1}$), and $\delta > 0$ is a chosen constant value. Usually in identification practice $\delta \in [0.01-0.1]$, which corresponds to a relative variation of prediction error standard deviation from 1% to 10%.

Coefficient estimates of polynomial $B(z^{-1})$ transfer function and nonlinear characteristics $f(x_t)$ of Hammerstein-type models (1)–(6) are connected with coefficient estimates of models (8)–(14) in the following way:

$$\hat{b}_j = \frac{K_w}{K_w^*} \hat{b}_j^*, \quad j = 0, 1, \dots, \hat{m}, \quad (45)$$

$$\hat{f}_0 = \frac{K_H}{K_W} \hat{\theta}_0, \quad (46)$$

$$\hat{f}_1 = \frac{K_W^*}{K_W}, \quad (47)$$

$$\hat{f}_2 = \frac{K_W^*}{K_W}, \tag{48}$$

where

$$K_W = \frac{\sum_{j=0}^m b_j}{1 + \sum_{i=1}^n a_i} \tag{49}$$

is a gain of a transfer function (2),

$$K_W^* = \frac{\sum_{j=0}^{\hat{m}} \hat{b}_j^*}{1 + \sum_{i=1}^{\hat{n}} \hat{a}_i} \tag{50}$$

is a gain of model (8) transfer function

$$W_*(z^{-1}) = \frac{\hat{B}_*(z^{-1})}{\hat{A}(z^{-1})}, \tag{51}$$

$$K_H = \frac{1}{1 + \sum_{i=1}^{\hat{n}} \hat{a}_i} \tag{52}$$

is a gain of a transfer function (3).

From (45)–(48) follows that the reconstruction of primary model parameter estimates requires a priori selection of gain K_W of Hammerstein-type model input channel transfer function. It is generally accepted that:

$$K_W = \begin{cases} 1, & \text{if } K_W^* > 0, \\ -1, & \text{if } K_W^* < 0. \end{cases} \tag{53}$$

In this case, from (47)–(48) follows that estimates of the coefficients f_1 and f_2 of (4) and (5) will be positive (functions $f(x_t)$ are symmetrically increasing with respect to the origin).

4. Validation of Models

Validation of the models (1)–(6) was performed for each of 7 volunteers (males and females). Each model is selected from nine possible models (when $n = 1, 2, 3$, and $m = 0, 1, 2, 3$) using the rules (39)–(41) when $\delta = 0.05$. The analysis of data showed that relations between distance-between-eyes input and excitement output signal can be modelled when model order is $\hat{m} = 0, \hat{n} = 1$, frustration output signal can be modelled when model order is $\hat{m} = 0, \hat{n} = 2$, and engagement/boredom output signal can be modelled when model order is $\hat{m} = 0, \hat{n} = 3$. These estimates are obtained when relative variation of prediction error standard deviation is 5%. According to data analysis results, one-step-ahead prediction of output signals for every model can be performed using the following

expressions (Kaminskas, 1985):

$$\begin{aligned}\hat{y}_{t+1|t} &= z[1 - \hat{A}(z^{-1})]y_t + \hat{B}(z^{-1})\hat{f}(x_{t+1}) \\ &= \sum_{j=0}^{\hat{m}} \hat{b}_j \hat{f}(x_{t+1-j}) - \sum_{i=1}^{\hat{n}} \hat{a}_i y_{t+1-i},\end{aligned}\quad (54)$$

$$\hat{f}(x_t) = \hat{f}_0 + \hat{f}_1 |x_t| \quad (55)$$

or

$$\hat{f}(x_t) = \hat{f}_0 + \hat{f}_2 x_t^2. \quad (56)$$

Prediction accuracies were evaluated using the following measures:

- prediction error standard deviation

$$\sigma_\varepsilon = \sqrt{\frac{1}{N} \sum_{t=0}^{N-1} (y_{t+1} - \hat{y}_{t+1|t})^2}, \quad (57)$$

- relative prediction error standard deviation

$$\tilde{\sigma}_\varepsilon = \sqrt{\frac{1}{N} \sum_{t=0}^{N-1} \left(\frac{y_{t+1} - \hat{y}_{t+1|t}}{y_{t+1}} \right)^2}, \quad (58)$$

- and average absolute relative prediction error

$$|\bar{\varepsilon}| = \frac{1}{N} \sum_{t=0}^{N-1} \left| \frac{y_{t+1} - \hat{y}_{t+1|t}}{y_{t+1}} \right| \times 100\%. \quad (59)$$

One-step-ahead predictions (54)–(56) were performed using the observation data that were used to parameter estimation ($M = 124$ in TYPE III stimulus case and $M = 80$ in TYPE I/II stimuli cases, in (20)) and the additional ones that were not used to parameter estimation (in total $N = 200$ in TYPE III stimulus case and $N = 110$ in TYPE I/II stimuli case, in (57)–(59)). Prediction accuracy measures are provided in Tables 1–3.

Figures 6–7 show examples of one-step-ahead prediction results when using models (1)–(6) for two volunteers. Thick solid line denotes an observed signal, thick dotted line denotes predicted signal and thin solid line denotes prediction error at every time moment. Vertical line denotes M position as model parameters were estimated in the interval from 0 to M (equal to 80 when input TYPE I is used). As sampling period $T_0 = 0.5$ s, M is 40 s.

Examples of parameter estimates of the models (54)–(56) are given in Tables 4–5.

Table 1
Prediction accuracy measures for input TYPE I.

Vol. no.	Output	$f(x_t) = f_0 + f_1 x_t $			$f(x_t) = f_0 + f_2x_t^2$		
		σ_ε	$\tilde{\sigma}_\varepsilon, \%$	$ \bar{\varepsilon} , \%$	σ_ε	$\tilde{\sigma}_\varepsilon, \%$	$ \bar{\varepsilon} , \%$
(1) female	Excitement	0.024	10.1	8.2	0.023	10.0	8.3
	Frustration	0.011	2.5	1.7	0.011	2.5	1.7
	Engagement	0.008	0.8	0.6	0.008	0.8	0.6
(2) male	Excitement	0.057	13.9	10.6	0.051	11.5	8.7
	Frustration	0.021	4.2	3.2	0.021	4.2	3.2
	Engagement	0.006	1.0	0.7	0.006	1.0	0.7
(3) male	Excitement	0.053	17.0	12.5	0.046	15.5	11.1
	Frustration	0.014	5.0	3.5	0.014	5.0	3.5
	Engagement	0.009	2.4	1.5	0.009	2.4	1.5

Table 2
Prediction accuracy measures for input TYPE II.

Vol. no.	Output	$f(x_t) = f_0 + f_1 x_t $			$f(x_t) = f_0 + f_2x_t^2$		
		σ_ε	$\tilde{\sigma}_\varepsilon, \%$	$ \bar{\varepsilon} , \%$	σ_ε	$\tilde{\sigma}_\varepsilon, \%$	$ \bar{\varepsilon} , \%$
(1) female	Excitement	0.024	9.1	7.2	0.024	9.1	7.2
	Frustration	0.011	2.5	1.9	0.011	2.5	1.9
	Engagement	0.014	1.7	1.3	0.014	1.7	1.3
(2) male	Excitement	0.060	17.9	13.4	0.060	18.9	14.2
	Frustration	0.024	7.1	5.2	0.024	7.1	5.2
	Engagement	0.010	2.0	1.5	0.010	2.0	1.5
(3) male	Excitement	0.066	10.2	7.9	0.066	10.0	7.8
	Frustration	0.11	2.8	2.3	0.11	2.8	2.3
	Engagement	0.008	2.1	1.5	0.008	2.1	1.5

Table 3
Prediction accuracy measures for input TYPE III.

Vol. no.	Output	$f(x_t) = f_0 + f_1 x_t $			$f(x_t) = f_0 + f_2x_t^2$		
		σ_ε	$\tilde{\sigma}_\varepsilon, \%$	$ \bar{\varepsilon} , \%$	σ_ε	$\tilde{\sigma}_\varepsilon, \%$	$ \bar{\varepsilon} , \%$
(4) female	Excitement	0.038	12.6	9.1	0.038	12.6	9.1
	Frustration	0.019	3.5	2.6	0.019	3.5	2.6
	Engagement	0.008	1.5	1.1	0.008	1.6	1.1
(5) male	Excitement	0.031	12.4	7.7	0.030	12.1	7.6
	Frustration	0.007	2.2	1.6	0.007	2.2	1.5
	Engagement	0.008	1.8	1.1	0.008	1.8	1.1
(6) female	Excitement	0.018	9.0	5.7	0.018	9.0	5.7
	Frustration	0.017	3.4	2.7	0.017	3.4	2.7
	Engagement	0.006	0.8	0.6	0.006	0.8	0.6
(7) male	Excitement	0.025	10.3	7.1	0.025	10.3	7.1
	Frustration	0.016	3.9	2.8	0.016	3.9	2.8
	Engagement	0.004	0.7	0.5	0.004	0.7	0.5

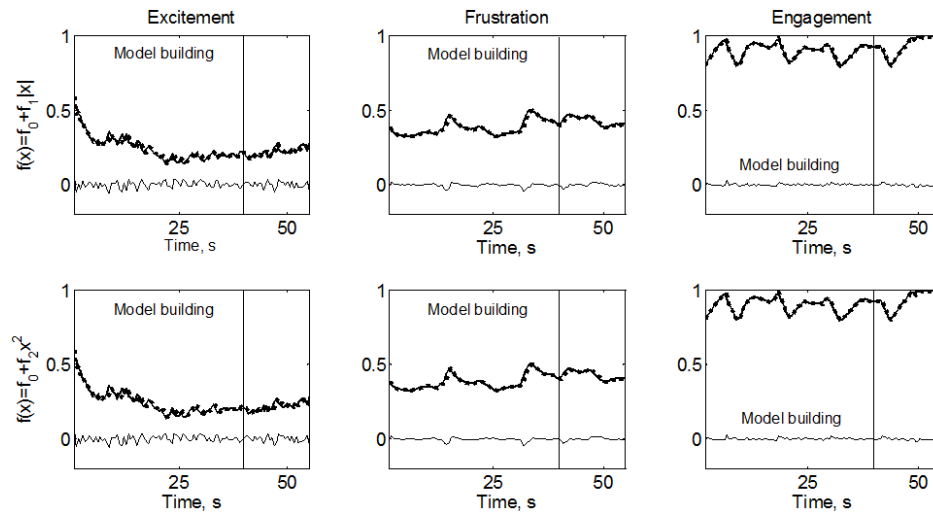


Fig. 6. One-step-ahead prediction results when using models (1)–(6) for volunteer no. 1 input TYPE I. Thick solid line denotes an observed signal, thick dotted line – predicted signal and thin solid line – prediction error.

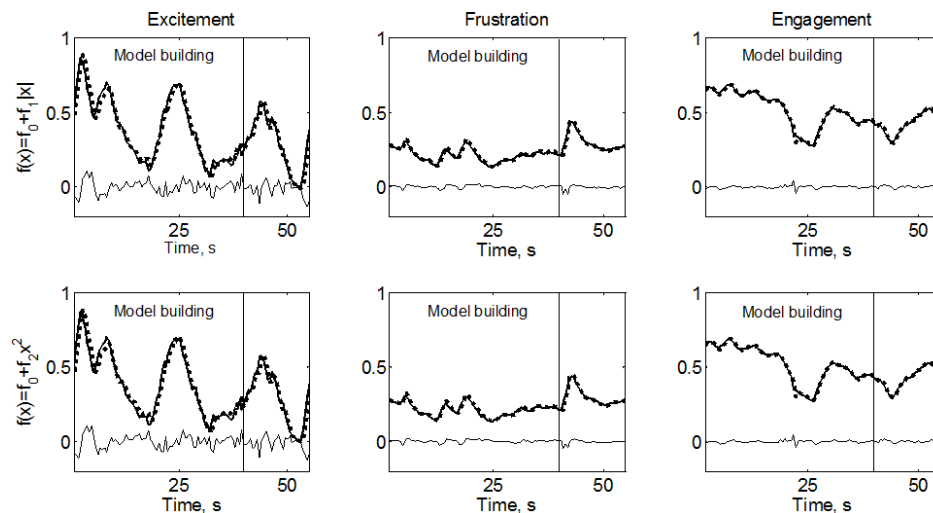


Fig. 7. One-step-ahead prediction results when using models (1)–(6) for volunteer no. 3 input TYPE I. Thick solid line denotes an observed signal, thick dotted line – predicted signal and thin solid line – prediction error.

Engagement/boredom signal was predicted with the least average absolute relative prediction error (less than 1.5%). Frustration signal was predicted with less than 5.2% average absolute relative prediction error. Excitement signal was predicted with the largest prediction error, but less than 14.2%. These models are more accurate than previously investigated linear models (Vaškevičius *et al.*, 2014). Average values of this prediction accuracy measure calculated from the results of ten experiments do not exceed 1% for engagement, 3% for frustration and 9% for excitement signal.

Table 4
Estimated parameters for excitement signal prediction using first order model $\hat{m} = 0, \hat{n} = 1$ for input TYPE I.

Volunteer no. 1 (female)			Volunteer no. 2 (male)		
$f(x_t)$:	$f_0 + f_1 x_t $	$f_0 + f_2x_t^2$	$f(x_t)$:	$f_0 + f_1 x_t $	$f_0 + f_2x_t^2$
\hat{b}_0	0.154	0.155	\hat{b}_0	-0.041	-0.041
\hat{a}_1	-0.846	-0.845	\hat{a}_1	-0.959	-0.959
\hat{f}_0	0.172	0.190	\hat{f}_0	-0.445	-0.651
\hat{f}_1	0.047	-	\hat{f}_1	0.142	-
\hat{f}_2	-	0.023	\hat{f}_2	-	0.248

Table 5
Estimated parameters for excitement signal prediction using first order model $\hat{m} = 0, \hat{n} = 1$ for input TYPE III.

Volunteer no. 6 (female)			Volunteer no. 7 (male)		
$f(x_t)$:	$f_0 + f_1 x_t $	$f_0 + f_2x_t^2$	$f(x_t)$:	$f_0 + f_1 x_t $	$f_0 + f_2x_t^2$
\hat{b}_0	-0.090	-0.090	\hat{b}_0	-0.110	-0.110
\hat{a}_1	-0.910	-0.910	\hat{a}_1	-0.890	-0.890
\hat{f}_0	-0.103	-0.102	\hat{f}_0	-0.275	-0.266
\hat{f}_1	0.007	-	\hat{f}_1	0.038	-
\hat{f}_2	-	0.003	\hat{f}_2	-	0.014

5. Conclusions

Two Hammerstein-type models (when non-linearity of the input channel do not go through the origin) were proposed to describe the dependencies between human emotional signals (excitement, frustration, and engagement/boredom) and 3D face feature (distance-between-eyes).

It is shown that using least squares method with projection to the stability domain allows building stable Hammerstein-type models for one-step-ahead predictions of excitement, frustration, and engagement/boredom signals with the smallest prediction errors.

The validation results with data collection from seven volunteers and three types of experiment plan show that excitement can be predicted on average with less than 9%, frustration – with less than 3% and engagement/boredom – with less than 1% average absolute relative prediction error. According to the prediction accuracies, two models (1)–(3), (4), (6) and (1)–(3), (5), (6) with different nonlinear characteristics (respectively absolute, and quadratic) of the input channel are similar.

References

Calvo, R.A., D’Mello, S.K., Gratch, J., Kappas, A. (2015). *The Oxford Handbook of Affective Computing*. Oxford library of Psychology, Oxford University Press, Oxford.

Emotiv EPOC specifications. *Brain-computer interface technology*. Available at: <http://www.emotiv.com/upload/manual/sdk/EPOCSpecifications.pdf>.

Graimann, B., Allison, B., Pfurtscheller, G. (2011). Brain-computer interfaces. Revolutionizing human-computer interaction. In: *The Frontiers Collection*. Springer-Verlag, Berlin, Heidelberg.

- Hondrou, C., Caridakis, G. (2012). Affective, natural interaction using EEG: sensors, application and future directions. In: *Artificial Intelligence: Theories and Applications*, Vol. 7297. Springer-Verlag, Berlin, Heidelberg, pp. 331–338.
- Jury, E.I. (1962). A simplified stability criterion for linear discrete systems. *Proceedings of the IRE*, 50, 1493–1500.
- Kaminskas, V. (1982). *Dynamic Systems Identification via Discrete-Time Observations*, Part 1. Mokslas, Vilnius (in Russian).
- Kaminskas, V. (1985). *Dynamic Systems Identification via Discrete-Time Observations*, Part 2. Mokslas, Vilnius.
- Kaminskas, V., Vaškevičius E., Vidugirienė, A. (2014). Modeling human emotions as reactions to a dynamical virtual 3D face. *Informatica*, 25(3), 425–437.
- Scherer, K.R., Baenziger, T., Roesch, E.B. (2010). *Blueprint for Affective Computing. A Sourcebook and Manual. Series in Affective Science*. Oxford University Press, Oxford.
- Sourina, O., Liu, Y. (2011). A fractal-based algorithm of emotion recognition from EEG using arousal-valence model. In: *Proceedings of the Biosignals*, pp. 209–214.
- Suprijanto, L., Sari, V., Nadhira, I.G.N., Merthayasa, I.M. Farida (2009). Development system for emotion detection based on brain signals and facial images. *World Academy of Science, Engineering and Technology*, 26, 931–938.
- Tan, D.S., Nijholt, A. (2010). Brain-Computer Interfaces. *Applying Our Minds to Human-Computer Interaction, Human-Computer Interaction Series*. Springer-Verlag, Berlin.
- Vaškevičius, E., Vidugirienė, A., Kaminskas, V. (2014). Identification of human response to virtual 3D face stimuli. *Information Technologies and Control*, 43(1), 47–56.
- Zisook, M., Hernandez, J., Goodwin, M.S., Picard, R.W. (2013). Enabling visual exploration of long-term physiological data. In: *Proceedings of the 2013 IEEE Conference on Visual Analytics Science and Technology*, USA, Georgia, Atlanta.

V. Kaminskas is the head of System Analysis Department of Vytautas Magnus University. He graduated from the Department of Automatics of the Kaunas Polytechnical Institute in 1968. He has PhD (1972) and DrSc (1983) degrees in the field of technical cybernetics and information theory. In 1984 he was awarded the title of Professor. From 1991 he is a member of Lithuanian Academy of Sciences. His research interests are dynamic system modelling, identification and adaptive control. He is the author of 4 monographs and about 200 scientific papers on these topics.

A. Vidugirienė is an associate professor at the Department of System Analysis, Faculty of Informatics, Vytautas Magnus University. She received a PhD degree (Informatics) in 2010 from Vytautas Magnus University, Kaunas, Lithuania. Her research interests concern emotion regulation modelling using bio-feedback, multimedia systems control using feedback, signal processing and prediction.

Netiesinių Hameršteino tipo modelių lyginimas identifikuojant žmogaus reakciją į virtualius trimačio veido stimulus

Vytautas KAMINSKAS, Aušra VIDUGIRIENĖ

Šiame straipsnyje pateikiamas dviejų netiesinių įėjimas-išėjimas tipo modelių, kurie aprašo sąryšius tarp žmogaus emocinių signalų (susijaudinimo, susierzinimo ir susidomėjimo / nuobodulio) ir virtualaus trimačio veido su besikeičiančiu atstumu tarp akių, lyginimas. Stabiliems modeliams su mažiausia išėjimo prognozės paklaida sudaryti pasiūlytas mažiausių kvadratų metodas su projekcija į stabilumo sritį. Validavimas buvo atliktas su septyniais savanoriais ir trimis įėjimo signalo tipais. Modeliavimo rezultatai parodė santykinai aukštus susijaudinimo, susierzinimo ir susidomėjimo / nuobodulio signalų prognozių tikslumus.